Antineutrophil Cytoplasmic Autoantibodies Interact with Primary Granule Constituents on the Surface of Apoptotic Neutrophils in the Absence of Neutrophil Priming

By Hannah M. Gilligan,*‡ Brunel Bredy,*‡ Hugh R. Brady,‖ Marie-Josée Hébert,¶ Henry S. Slayter,** Yuhui Xu,** Joyce Rauch,‡‡ Michael A. Shia,*§ Jason S. Koh,*‡ and Jerrold S. Levine*‡

*From the *Renal Section, Evans Memorial Department of Clinical Research, and ‡Department of Medicine and §Department of Biochemistry, Boston University Medical Center Hospital, Boston, Massachusetts 02118; ‖Department of Medicine and Therapeutics, University College Dublin, Mater Miseracordiae, Dublin 7, Ireland; ¶Renal Division, Department of Medicine, Brigham and Women's Hospital, and the Renal Section, Medical Service, Brockton-West Roxbury Department of Veterans Affairs Medical Center, Harvard Medical School, Boston, Massachusetts 02132; **Laboratories of Electron Microscopy and Structural Molecular Biology, Dana Farber Cancer Institute, and Department of Cellular and Molecular Physiology, Harvard Medical School, Boston, Massachusetts 02132; and ‡‡Division of Rheumatology, Montreal General Hospital Research Institute, McGill University, Montreal, QC, Canada H3G 1A4*

Summary

The pathogenic role of antineutrophil cytoplasmic autoantibodies (ANCA) remains controversial because of the difficulty in explaining how extracellular ANCA can interact with intracellular primary granule constituents. It has been postulated that cytokine priming of neutrophils (PMN), as may occur during a prodromal infection, is an important trigger for mobilization of granules to the cell surface, where they may interact with ANCA. We show by electron microscopy that apoptosis of unprimed PMN is also associated with the translocation of cytoplasmic granules to the cell surface and alignment just beneath an intact cell membrane. Immunofluorescent microscopy and FACS® analysis demonstrate reactivity of ANCA-positive sera and antimyeloperoxidase antibodies with apoptotic PMN, but not with viable PMN. Moreover, we show that apoptotic PMN may be divided into two subsets, based on the presence or absence of granular translocation, and that surface immunogold labeling of myeloperoxidase occurs only in the subset of PMN showing translocation. These results provide a novel mechanism that is independent of priming, by which ANCA may gain access to PMN granule components during ANCA-associated vasculitis.

Antineutrophil cytoplasmic autoantibodies (ANCA)[1] are associated with systemic vasculitides, especially Wegener's granulomatosis and microscopic polyarteritis (1–4). ANCA are also seen with idiopathic crescentic glomerulonephritis without immune deposits (2), and several other inflammatory or rheumatic diseases (3, 4). These autoAb are mainly directed against proteins in PMN primary granules and monocyte lysosomes (5). When detected by indirect immunofluorescence (IF) of ethanol-fixed PMN, there are two major patterns of ANCA staining—cytoplasmic (C-ANCA) and perinuclear (P-ANCA) (2). The major C-ANCA Ag is proteinase 3 (PR3) (6), a 29 kD serine proteinase. The major P-ANCA Ag is myeloperoxidase (MPO) (2). Although PR3 and MPO are located in the primary granules of PMN, ethanol fixation leads to solubilization and nuclear redistribution of MPO, leading to an artifactual perinuclear staining pattern (2, 7). Other minor ANCA Ag have been described, leading to both C- and P-ANCA patterns, but these account for <5% of positive ANCA (5).

The pathogenic role of ANCA remains controversial, in part because it is difficult to explain how extracellular ANCA interact with intracellular primary granule components. Al-

[1]*Abbreviations used in this paper:* ANCA, antineutrophil cytoplasmic autoantibodies; C-ANCA, ANCA with cytoplasmic staining pattern on indirect immunofluorescence; CHX, cycloheximide; EM, electron microscopy; GBM, glomerular basement membrane; IF, immunofluorescence; MPO, myeloperoxidase; P-ANCA, ANCA with perinuclear staining pattern on indirect immunofluorescence; PI, propidium iodide; PR3, proteinase 3.

 J. Exp. Med. © The Rockefeller University Press • 0022-1007/96/12/2231/11 $2.00
Volume 184 December 1996 2231–2241

though several models have been put forth (8–10), most authors invoke some "priming" event by which the PMN is preactivated (11), whereby primary granules translocate to the cell surface without releasing their contents. Priming may occur in vivo during a prodromal infection or other inflammatory process (12), and can be induced in vitro by various cytokines (e.g., TNF-α), LPS, or chemotactic factors (10, 11, 13). ANCA can activate primed PMN in vitro, leading to degranulation and release of reactive oxygen species (10, 13, 14).

We present data supporting an alternative model in which PMN priming need not be invoked. PMN are short-lived cells, having a circulatory half-life of several days. Death occurs by apoptosis (15), an energy-requiring process that leads to cellular "suicide" (16). We show that PMN apoptosis is associated with translocation of cytoplasmic granules to the cell surface, thereby leading to increased reactivity with anti-MPO Ab and ANCA sera. Our results suggest a novel mechanism that is independent of priming, by which ANCA may interact with PMN granule components during ANCA-associated vasculitis.

Materials and Methods

Materials. Ficoll-Hypaque (Lymphocyte Separation Medium) was obtained from Organon Technika (Durham, NC), bisbenzamide (Hoechst dye or H-33342) from Molecular Probes, Inc. (Eugene, OR), dextran from Pharmacia AB (Uppsala, Sweden), polyclonal rabbit anti–human MPO Ab from Calbiochem-Novabiochem Corp. (La Jolla, CA), FITC-conjugated goat anti–rabbit IgG from Cappel Laboratories (Durham, NC); FITC-conjugated goat anti–human IgG (Fc-specific) from Incstar Co. (Stillwater, MN); gold-conjugated (10 nm) goat anti–rabbit IgG from Ted Pella, Inc. (Redding, CA); and RPMI 1640 medium and penicillin-streptomycin solution from GIBCO BRL (Gaithersburg, MD). All other materials, including BSA, propidium iodide (PI), cycloheximide (CHX), and Dulbecco's PBS with calcium and magnesium chloride (PBS^+), were obtained from Sigma Chemical Co. (St. Louis, MO).

Patients. ANCA sera ($n = 10$) and sera from patients with anti–glomerular basement membrane (anti-GBM) disease ($n = 2$) were a gift from Dr. John Niles (Massachusetts General Hospital, Boston, MA). ANCA staining patterns were determined by indirect IF on ethanol-fixed normal human PMN (17). As confirmed by ELISA (18), the antigenic specificity of all P-ANCA sera ($n = 5$) was MPO, and that of all C-ANCA sera ($n = 5$) was PR3. P-ANCA sera showed no cross-reactivity for PR3, and C-ANCA sera showed no cross-reactivity for MPO. All ANCA sera were of high titer (>100 U of activity; 17). For anti-GBM sera, autoreactivity for the noncollagenous domain of type IV collagen (Goodpasture epitope) was confirmed by Western blotting, with no cross-reactivity for ANCA Ag. Normal sera ($n = 12$) were obtained from healthy volunteers. All sera were heat-inactivated for 1 h at 56°C before use.

Isolation and Culture of PMN. PMN were isolated from heparinized venous blood from healthy volunteers by standard techniques of Ficoll-Hypaque density gradient centrifugation and dextran sedimentation (19). PMN were suspended in culture medium (RPMI 1640 with 10% heat-inactivated human serum and 1% penicillin–streptomycin solution).

Resultant suspensions contained ≥95% PMN, as assessed by cytospin and Wright-Giemsa staining. Viability was ≥99%, as assessed by trypan blue exclusion. Importantly, other investigators have shown that this technique yields PMN with a quiescent phenotype under basal conditions by multiple criteria: (*a*) low levels of heterotypic adhesion (20); (*b*) no superoxide anion generation (21); (*c*) no generation of 5-lipoxygenase–derived eicosanoids (22); and (*d*) L-selectin expression with relatively low levels of CD11b/CD18 (data not shown). Upon receptor-triggered stimulation, PMN upregulate CD11b/CD18, shed L-selectin, show increased adhesiveness for endothelial cells, and generate reactive oxygen species and 5-lipoxygenase products (19–22).

Induction of Apoptosis. Freshly isolated PMN were cultured at $1–2 \times 10^6$ cells/ml and were incubated for 18 h at 37°C in a humidified atmosphere containing 5% CO_2. PMN were incubated under identical conditions with CHX (10 μg/ml) to induce increased apoptosis (23).

IF Staining with Human Sera. After induction of apoptosis, PMN were cooled to 4°C, washed in PBS^+, and suspended in staining medium (RPMI 1640, 1% BSA, 25 mM Tris, pH 8.3). PMN were then treated with serum at a constant ratio of 50 μl serum per $1–2 \times 10^6$ cells for 60 min. Bound Ab was detected with FITC-conjugated goat anti–human IgG at a 1:20 dilution in staining medium. All incubations were performed at 4°C to prevent capping and shedding of bound Ab. PMN were then treated

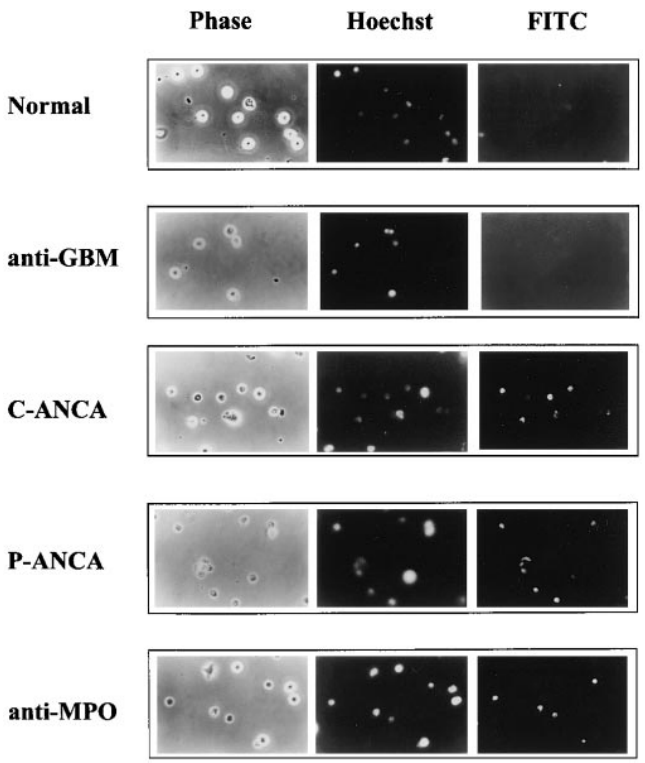

Figure 1. ANCA bind to the surface of unprimed apoptotic PMN. Unprimed apoptotic PMN were treated with polyclonal anti-MPO Ab, normal serum, anti-GBM serum, and high titer C- and P-ANCA sera. Cells were photographed under epifluorescence microscopy for Hoechst, PI, and FITC. All cells excluded PI and so had intact cell membranes. Apoptotic PMN with nuclear condensation comprised two distinct subpopulations with bright or faint Hoechst staining. Surface FITC staining of apoptotic PMN by ANCA sera and anti-MPO Ab occurred more commonly in apoptotic PMN with fainter Hoechst staining.

with Hoechst dye for 10 min at 37°C and placed on ice. Hoechst dye, a cell-permeant supravital DNA stain, identified the condensed chromatin characteristic of apoptotic cells (24). PI was added immediately before IF microscopy or FACS® analysis (Becton Dickinson & Co., Mountain View, CA). Permeant cells, identified by uptake of PI, were excluded from IF and FACS® studies.

Viable PMN were defined as PI negative with faint nuclear Hoechst staining. Apoptotic PMN were defined as PI negative with bright nuclear Hoechst staining. By these criteria, when PMN were incubated without CHX, 28.0 ± 9.0% were viable and 54.7 ± 11.4% were apoptotic. When PMN were incubated with CHX, 17.5 ± 8.3% were viable and 54.7 ± 11.7% were apoptotic. The remaining PMN in each case were PI positive and therefore excluded. The vast majority of excluded cells were smaller than viable PMN and likely represented apoptotic PMN that had progressed to postapoptosis (or secondary necrosis). Necrotic cells, identified by increased cell size and PI uptake, regularly comprised <1% of the final cell population.

IF Staining with Polyclonal Anti-MPO Ab. PMN suspensions were treated with polyclonal rabbit anti-human MPO Ab at a 1:50 or 1:100 dilution (2 μl per 1-2 × 10^6 cells) in staining medium. Bound Ab was detected with FITC-conjugated goat anti–rabbit IgG at a 1:64 dilution. In all other aspects, the protocols for staining PMN with anti-MPO Ab or human sera were identical.

IF Microscopy and FACS® Analysis. Cells were photographed under epifluorescence microscopy for visualizing Hoechst, PI, and FITC staining in the same cells. FACS® analysis was performed on an Epics ESP Flow Cytometer (Coulter Electronics, Hialeah, FL) with an UV-enhanced argon laser. Hoechst fluorescence was performed by excitation with <5 mW of UV laser light (351–364 nm multiline). PI and FITC fluorescence were performed with 15 mW of 488 nm blue laser light. A gated amplifier option allowed spatial beam separation leading to minimal spectral overlap among Hoechst, PI, and FITC fluorescence. Detection of Hoechst, PI, and FITC fluorescence was achieved using 405-, 525-, and 575-nm bandpass optical filters, respectively. Data were analyzed by Epic Elite software (Coulter Electronics).

FACS® Sorting of PMN. PMN were stained with polyclonal anti-MPO Ab as described above. Populations of PMN within specific clusters (high FITC vs. low FITC staining) were sorted at a flow rate of 800–1,000 cells/s.

Assessment of PMN Morphology by Electron Microscopy. Sorted PMN were centrifuged at 500 *g* for 15 min, fixed with 2.5% glutaraldehyde in PBS for 1 h at 4°C, and washed three times in Sabatini's solution (PBS with 6.8% sucrose). Samples were postfixed with 1% osmium tetroxide (1 h), washed three times in Sabatini's solution, passed through a graded series of alcohols (30, 50, 70, 90, and 100% for 15 min each), and treated with propylene oxide (15 min), a 1:1 Epon-propylene oxide mix (1 h), and three changes

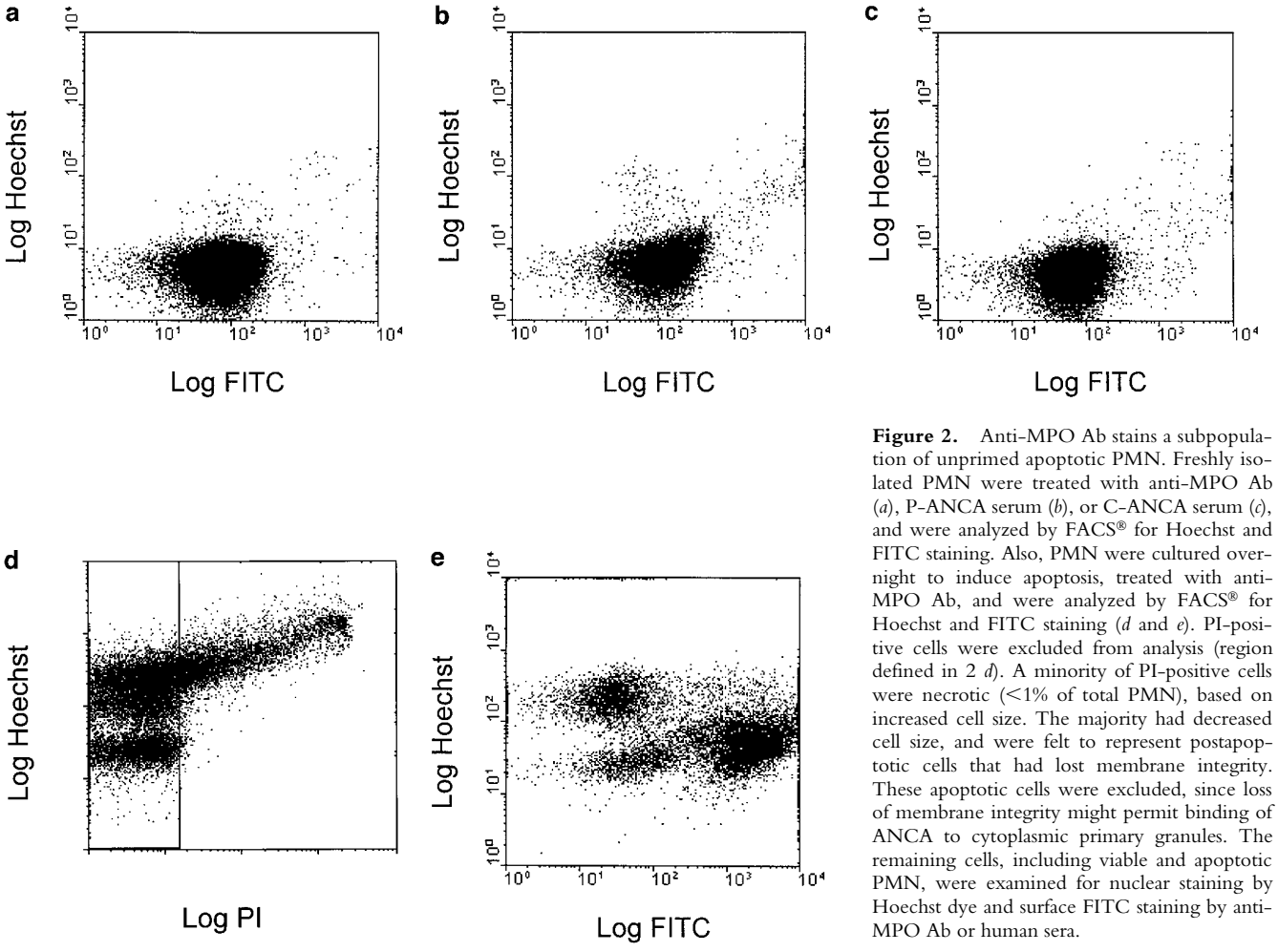

Figure 2. Anti-MPO Ab stains a subpopulation of unprimed apoptotic PMN. Freshly isolated PMN were treated with anti-MPO Ab (*a*), P-ANCA serum (*b*), or C-ANCA serum (*c*), and were analyzed by FACS® for Hoechst and FITC staining. Also, PMN were cultured overnight to induce apoptosis, treated with anti-MPO Ab, and were analyzed by FACS® for Hoechst and FITC staining (*d* and *e*). PI-positive cells were excluded from analysis (region defined in 2 *d*). A minority of PI-positive cells were necrotic (<1% of total PMN), based on increased cell size. The majority had decreased cell size, and were felt to represent postapoptotic cells that had lost membrane integrity. These apoptotic cells were excluded, since loss of membrane integrity might permit binding of ANCA to cytoplasmic primary granules. The remaining cells, including viable and apoptotic PMN, were examined for nuclear staining by Hoechst dye and surface FITC staining by anti-MPO Ab or human sera.

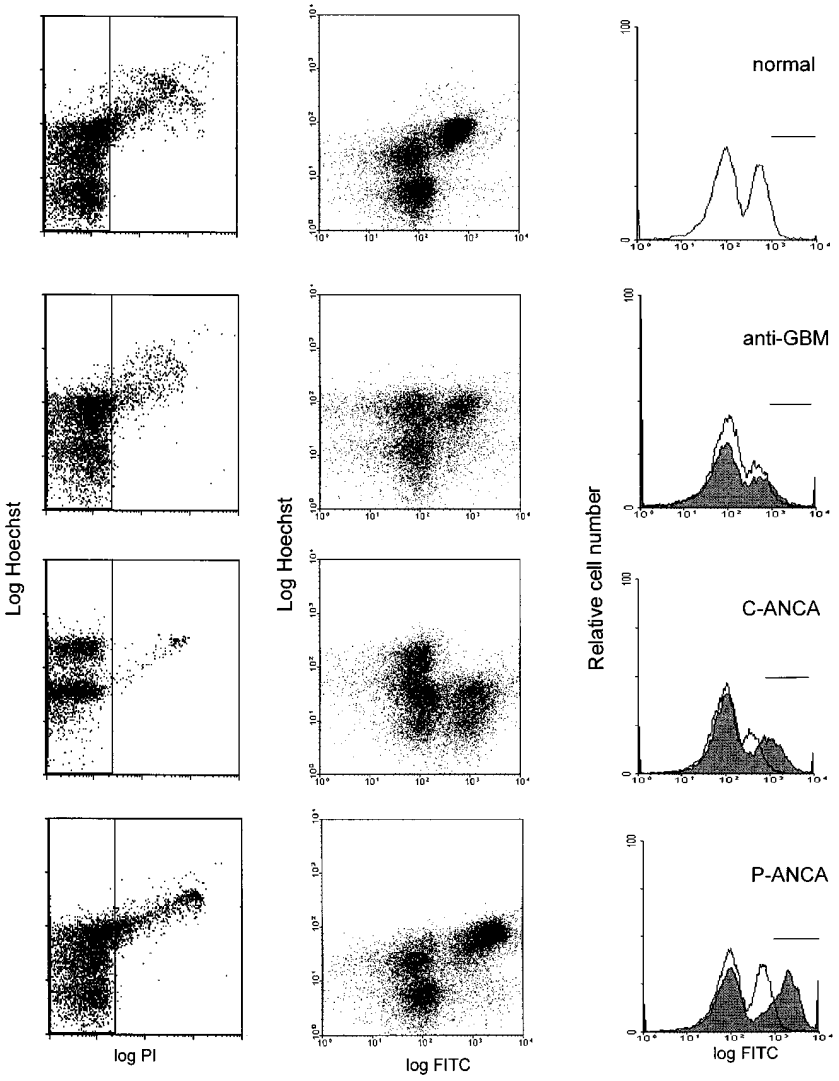

Figure 3. ANCA sera stain a subpopulation of unprimed apoptotic PMN. Apoptotic PMN were treated with anti-MPO Ab, normal serum, anti-GBM serum, and C-ANCA and P-ANCA sera. PMN, selected as described in the legend of Fig. 2, were examined for Hoechst and surface FITC staining. Left-hand panels depict scatter plots of Hoechst vs. PI staining. Middle panels are gated to include only PI-negative cells, and depict scatter plots of Hoechst vs. FITC staining. Shaded histograms in the right-hand panels are derived from the scatter plots and depict relative cell number as a function of log FITC fluorescence. Unshaded histograms represent control data from healthy volunteers.

in pure Epon (3 h, 3 h, and overnight). Polymerization occurred overnight at 64°C. Ultrathin sections (~50 nm) were cut with MT2 Sorvall ultramicrotome, stained with lead citrate and uranyl citrate, and examined by transmission electron microscopy (EM) (100CX; JEOL U.S.A. Inc., Peabody, MA) at 60 kV using a 20-μm objective aperture.

Preembedding Immunogold Staining of PMN for EM. PMN were washed in PBS and resuspended in PBS with 1% egg albumin. After a 10-min incubation on ice, PMN were centrifuged at 500 *g* for 15 min and resuspended in PBS with 0.5% egg albumin. Polyclonal rabbit anti–human MPO Ab was added at 1:50 dilution, and PMN were incubated on ice for 30 min. After three washes in PBS, PMN were treated with gold-conjugated goat anti–rabbit IgG at a 1:10 dilution for 30 min on ice. After three washes in PBS, PMN were centrifuged at 500 *g* for 15 min and fixed by slowly adding 1.25% glutaraldehyde in 0.1 M cacodylate buffer without disturbing the pellet. Processing for transmission EM was performed as indicated above for sorted PMN.

Statistics. Individual sera were tested at least twice on separate days with consistent results. Data are presented as the mean ± SD of the two experiments. Statistical significance was determined by a two-tailed Student's *t* test.

Results

ANCA Bind to the Surface of Unprimed Apoptotic PMN. Initial IF studies used high titer sera for P-ANCA and C-ANCA. To ensure that PMN isolation did not induce priming or activation, we incubated freshly isolated PMN with both ANCA sera. No surface staining of PMN was observed (not shown). Additional evidence confirming that isolation and culture of PMN did not induce priming or activation is given below.

To assess potential translocation of primary granule constituents to the cell surface during apoptosis, we incubated ANCA sera with PMN that had been cultured overnight to induce apoptosis. Both P-ANCA and C-ANCA sera bound specifically to the surface of apoptotic PMN, as shown by a correlation between surface FITC staining and the presence of condensed chromatin in PI-negative PMN (Fig. 1). Apoptotic PMN treated with anti-MPO Ab gave a similar staining pattern. In contrast, minimal staining occurred for apoptotic PMN that were incubated with normal or anti-GBM sera.

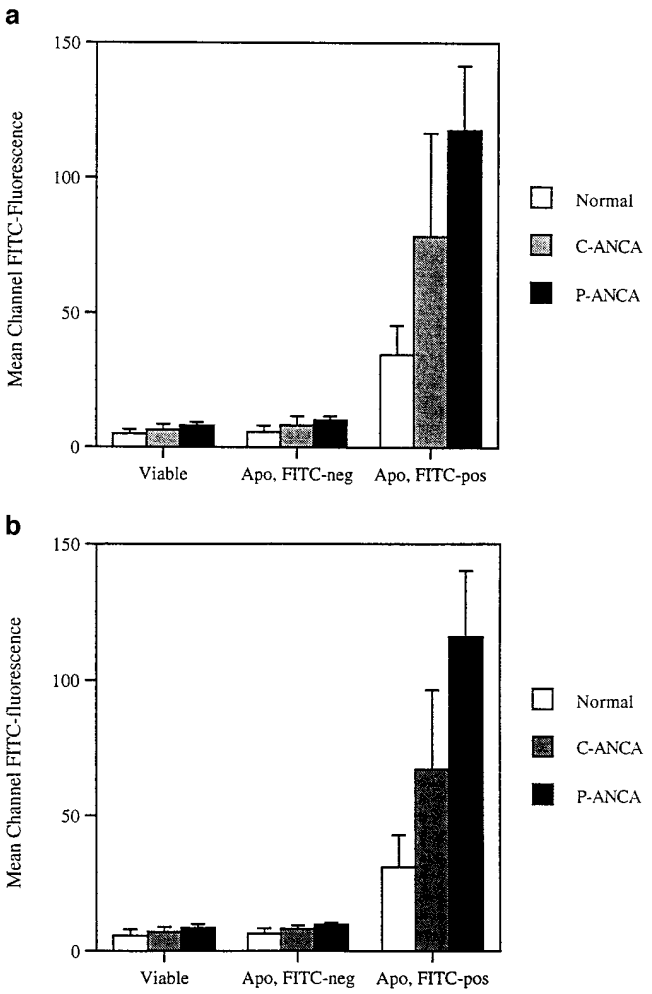

Figure 4. ANCA sera stain a subpopulation of unprimed apoptotic PMN. PMN apoptosis was induced by overnight culture with (*a*) or without (*b*) CHX. Scatter plots were gated into the same three subpopulations shown in Fig. 3. Mean channel FITC fluorescence for each subpopulation was compared among normal sera (n = 12), C-ANCA sera (n = 5), and P-ANCA sera (n = 5). PMN were selected as described in the legend of Fig. 2.

Surface Staining with ANCA Sera Is Restricted to a Subpopulation of Apoptotic PMN. Three-color FACS® analysis confirmed and extended these observations. Freshly isolated PMN treated with anti-MPO Ab yielded a single population with low Hoechst and low FITC staining (Fig. 2 *a*). Incubation with normal serum (not shown) or P-ANCA (Fig. 2 *b*) and C-ANCA (Fig. 2 *c*) sera also yielded a single population with low Hoechst and low FITC staining. In contrast, PMN that had been cultured overnight to induce apoptosis and treated with anti-MPO Ab comprised three distinct populations (Fig. 2 *d*): (*a*) a low Hoechst and low FITC population, likely representing viable PMN, based on similar staining to freshly isolated PMN; (*b*) a bright Hoechst and low FITC population corresponding to apoptotic PMN in Fig. 1 that were not recognized by anti-MPO Ab; and (*c*) a bright Hoechst and high FITC population representing apoptotic PMN that apparently express MPO on their

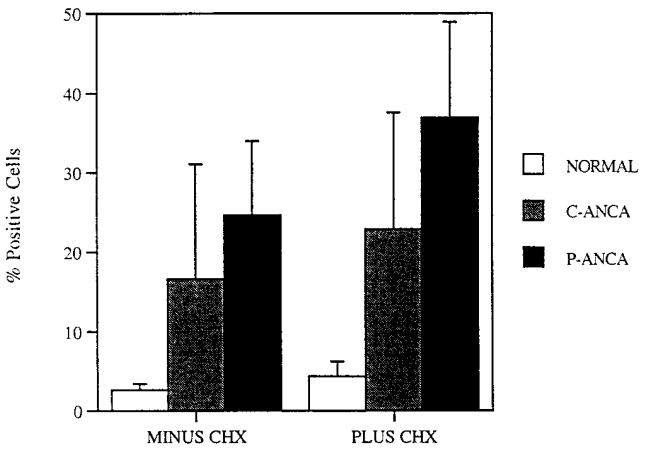

Figure 5. Surface staining of unprimed apoptotic PMN correlates with the presence of ANCA. PMN apoptosis was induced as described in the legend of Fig. 4. Positively staining PMN were defined as cells whose log-FITC fluorescence was greater than a threshold equal to the mean channel fluorescence with normal human sera for the high-FITC apoptotic population plus five standard deviations (see Fig. 4). Horizontal bars in the right-hand panels of Fig. 3 indicate the regions of positive log FITC fluorescence. PMN staining was compared among normal sera (n = 12), C-ANCA sera (n = 5), and P-ANCA sera (n = 5). PMN were selected as described in the legend of Fig. 2.

cell surface. Three similar populations were observed when apoptotic PMN were treated with P-ANCA and C-ANCA sera, anti-GBM serum, or normal serum (Fig. 3).

These observations were confirmed using pooled data from P-ANCA (n = 5) or C-ANCA (n = 5) sera. Data were analyzed in two ways. First, we compared the mean channel FITC fluorescence for each of the three PMN populations (Fig. 4). The mean channel fluorescence for P-ANCA and C-ANCA sera did not differ from that for normal sera (n = 12) among the viable or low FITC apoptotic populations. In contrast, among high-FITC apoptotic PMN, the mean channel fluorescences for P-ANCA and C-ANCA sera were ~4× (P <0.002) and 2× (P <0.05) that for normal sera. Identical results were obtained when apoptosis was induced with (Fig. 4 *a*) or without (Fig. 4 *b*) CHX.

Second, we determined the percentage of total PMN that showed surface FITC staining above a threshold level of fluorescence, defined by the horizontal bars in Fig. 3. For PMN cultured without CHX, the percentage of positive cells was 2.7 ± 0.8% for normal sera, 16.6 ± 14.5% for C-ANCA sera (P <0.1), and 24.6 ± 9.3% for P-ANCA sera (P <0.01) (Fig. 5). For PMN cultured with CHX, the percentage was 4.4 ± 1.9% for normal sera, 22.9 ± 14.7% for C-ANCA sera (P <0.05), and 36.9 ± 12.0% for P-ANCA sera (P <0.005) (Fig. 5).

Several points merit emphasis. First, surface FITC staining of viable PMN did not differ between ANCA-positive and ANCA-negative sera. Combined with the data shown in Fig. 2, these results imply that neither isolation nor culture of PMN induced priming. Thus, recognition of apoptotic PMN by ANCA sera may be specific to the apoptotic process. Second, surface staining by ANCA sera is seen

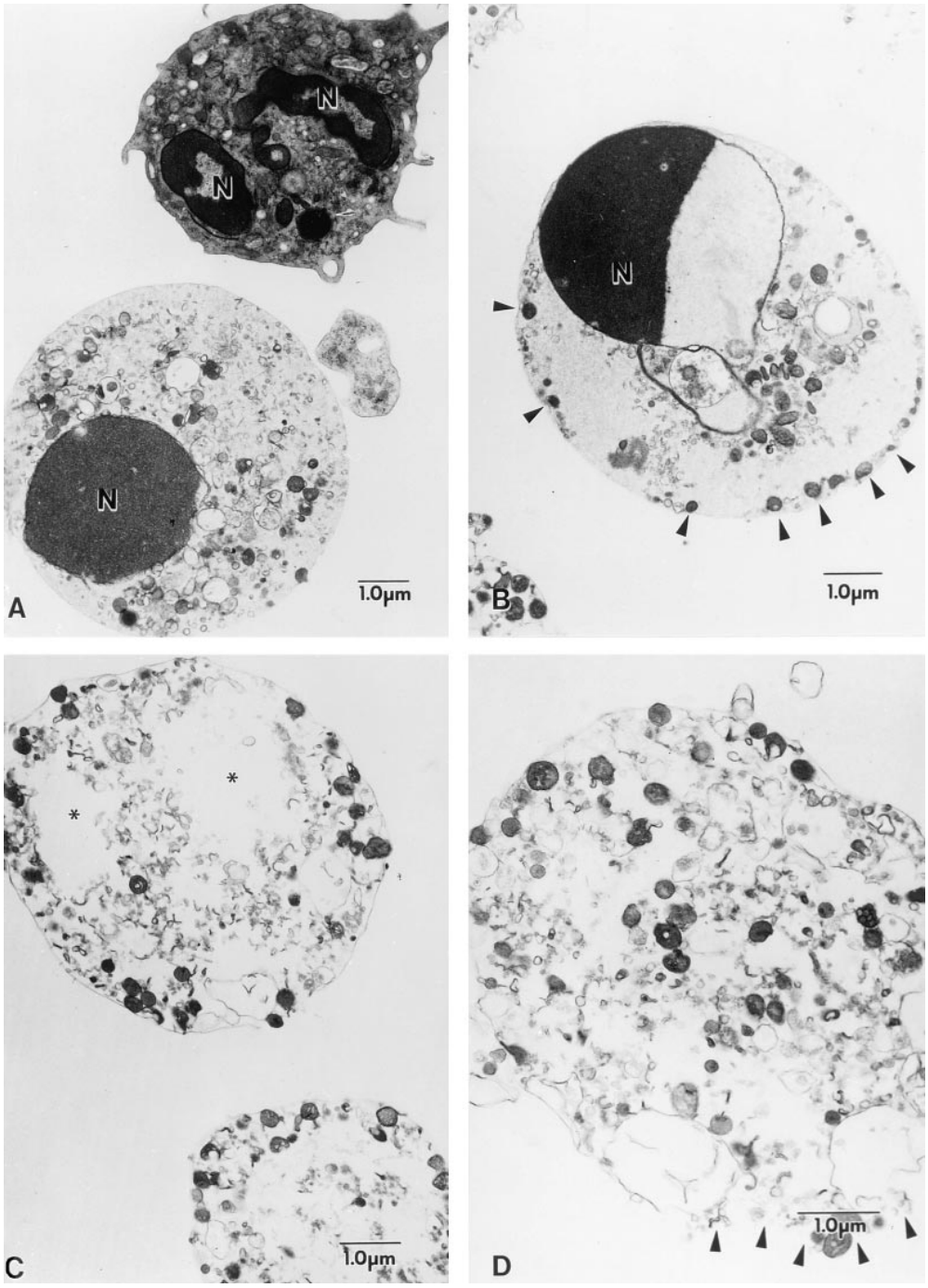

Figure 6. Cytoplasmic granules translocate to the cell surface during apoptosis. PMN, cultured overnight with CHX, were stained with anti-MPO Ab and sorted into two populations by FITC staining. (*A*) Low FITC staining. Shown are a viable (*upper*) and an apoptotic PMN (*lower*). The viable PMN has a multisegmented nucleus (*N*), many granules throughout the cytoplasm, and an irregular cell outline with membrane ruffling. The apoptotic PMN shows coalescence of the nuclear lobes, preservation of cytoplasmic granules, and a smooth rounded cell outline. (*B*) High-FITC staining. Shown is an apoptotic PMN sharing many features of apoptosis as within the low-FITC population, except for fewer cytoplasmic granules, many aligned just beneath an intact cell membrane (*arrow heads*). (*C*) High FITC staining. Shown are two apoptotic PMN, with nuclear disintegration (*) and decreased numbers of cytoplasmic granules, many again aligned beneath an intact cell membrane. (*D*) High-FITC staining. Shown is an apoptotic PMN with nuclear disintegration and loss of cell membrane integrity (*arrow heads*). This PMN is postapoptotic. Original magnifications: (*A*) ×8,700; (*B* and *C*) ×10,800; (*D*) ×15,000.

only in a subpopulation of apoptotic PMN. In fact, recognition of apoptotic PMN by ANCA sera seems to be an "all-or-nothing" phenomenon. Apoptotic PMN not recognized by ANCA displayed low FITC staining comparable to that of viable PMN. Thus, recognition of apoptotic PMN by ANCA sera appears to define a specific stage or morphologic feature of apoptosis, and only within this specific subpopulation of PMN does binding by ANCA sera differ from that by ANCA-negative sera. Finally, the existence of the same three populations using normal and anti-GBM sera suggests that the subpopulation of apoptotic PMN recognized by ANCA sera may be characterized by additional surface changes besides expression of MPO or PR3. Such changes may include decreased surface charge, decreased lectin binding sites, membrane reorganization, and/or altered surface ultrastructure (15, 25, 26).

Primary Granules Translocate to the PMN Cell Surface During Apoptosis. To determine directly whether surface stain-

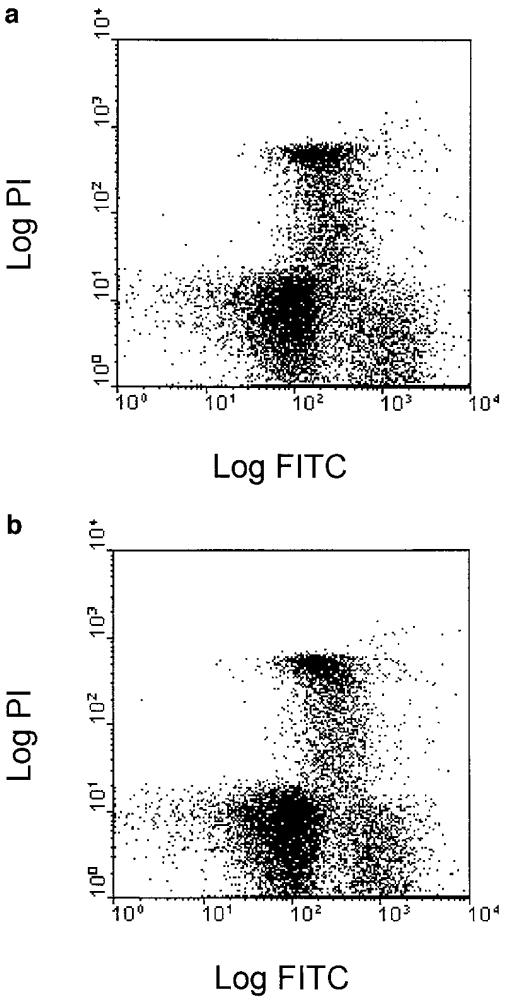

Figure 7. PMN apoptosis leads to decreased cellular content of ANCA Ag. PMN were cultured overnight, treated with P-ANCA (*a*) or C-ANCA (*b*) sera, and then analyzed by FACS® for PI and FITC staining. All PMN were included.

ing by ANCA sera reflected primary granule translocation, we sorted PMN into two populations by the level of FITC staining and assessed their morphology by EM.

The low FITC population contained two phenotypes. Viable PMN had typical morphologic features of mature PMN, including intact cell and nuclear membranes, multisegmented nuclei, granular appearance of the nuclear chromatin, large numbers of cytoplasmic granules, and an irregular cell outline characterized by membrane ruffling. Apoptotic PMN within the low FITC population showed classic features of apoptosis (15, 25, 27), including coalescence of the nuclear lobes into a single body, condensed chromatin, preservation of cytoplasmic granules, maintenance of cell membrane integrity, and a smooth rounded cell outline. Representative examples of a viable and FITC-negative apoptotic PMN are shown in Fig. 6 *a*.

The high FITC population also contained two phenotypes, both apoptotic. The first resembled apoptotic PMN found in the low FITC population, except for fewer cytoplasmic granules, many being aligned just beneath an intact cell membrane (Fig. 6 *b*). The second represented a later phase of apoptosis, characterized by nuclear disintegration, maintenance of cell membrane integrity, and diminished numbers of cytoplasmic granules, many again aligned just beneath the cell membrane (Fig. 6 *c*). Recent data suggest that disintegration of nuclear material may comprise a later step in PMN apoptosis before loss of membrane integrity (27). Loss of nuclear structure offers an explanation for the observation noted above, that surface FITC staining of apoptotic PMN correlates with less bright Hoechst staining. The high-FITC population also contained PMN with nuclear disintegration in association with loss of cell membrane integrity. Shedding of primary granules from these cells can be seen in areas of membrane integrity loss (Fig. 6 *d*).

PMN Apoptosis Is Associated with Diminished Cellular Content of ANCA Ag

Given these morphologic features, we hypothesized that translocated primary granules may be shed from the cell surface in the form of membrane-enclosed apoptotic bodies. Thus, when apoptosis has progressed to the stage of nuclear disintegration and loss of membrane integrity, there should be diminished numbers of primary granules within the cytoplasm. To test this, we regated selected FACS® analyses to include all apoptotic PMN, irrespective of PI entry, and assessed FITC staining in relation to PI staining (Fig. 7 *a* and *b*). Three distinct populations were observed: (*a*) a PI-negative and low FITC population comprised of viable PMN and apoptotic PMN whose primary granules have not yet undergone translocation; (*b*) a PI-negative and high FITC population comprised of apoptotic PMN with granular translocation; and (*c*) a PI-positive and intermediate FITC population (consistent with loss of primary granules) containing apoptotic PMN that have progressed to postapoptosis (see Fig. 9). This result is noteworthy in that FITC staining within the PI-positive population reflects the full complement of primary granules, both surface and cytoplasmic, whereas FITC staining within the PI-negative population represents only those granules that have undergone translocation.

Immunogold Labeling Localizes MPO on the Surface of Apoptotic PMN. To confirm ANCA binding to the apoptotic PMN surface and determine the ultrastructural site of binding, we used gold-conjugated anti–rabbit IgG to detect bound rabbit anti-MPO Ab. We restricted labeling to the cell surface by fixing PMN only after treatment with both Ab. Surface labeling was seen for the same two phenotypes of apoptotic PMN identified by high FITC sorting. These included early apoptotic PMN whose primary granules had translocated to the cell surface (Fig. 8 *B*) and late apoptotic PMN that had undergone nuclear disintegration (Fig. 8 *A*). Gold particles were localized over primary granules, as well as within "puffs" extending from the cell surface. The absence of gold particles within the cytoplasm attests to the preservation of membrane integrity during processing. Cytoplasmic staining may be seen in an apoptotic cell with

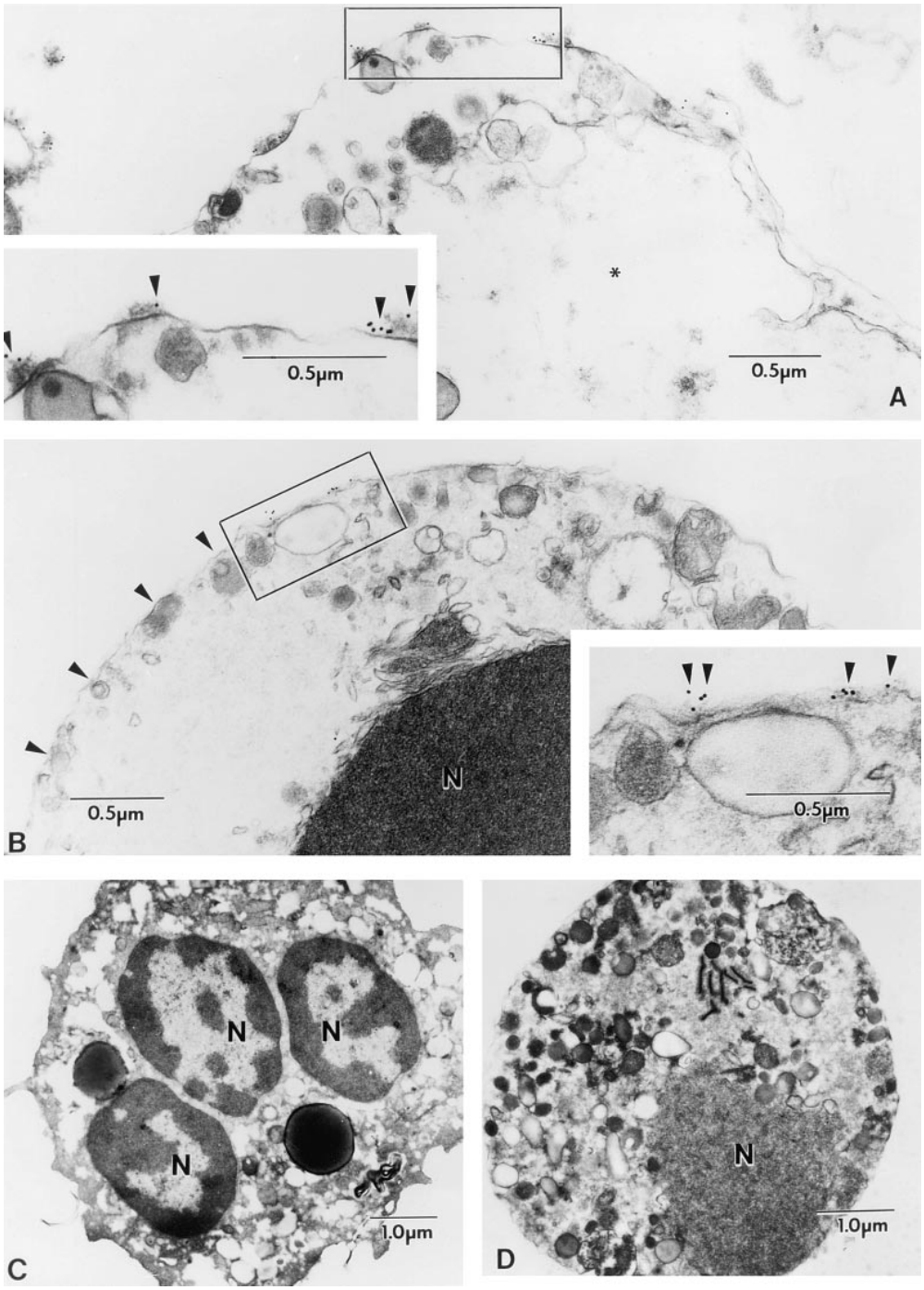

Figure 8. Immunogold labeling localizes MPO on the surface of apoptotic PMN. PMN were cultured overnight with CHX and treated with anti-MPO Ab, followed by gold-conjugated anti–rabbit IgG. To restrict labeling to the PMN surface, fixation occurred after treatment with both Ab. (*A* and *B*) Two apoptotic PMN with surface gold labeling. Both show decreased numbers of cytoplasmic granules, many aligned beneath an intact cell membrane (*arrow heads*). The PMN in *B* has a coalesced nucleus (*N*), whereas that in *A* has undergone nuclear disintegration (*). Boxed areas, showing areas of surface gold labeling, are enlarged within insets. These PMN are representative of the same two phenotypes sorted into the high FITC population for Fig. 6. (*C*) No surface gold labeling occurs on viable PMN. (*D*) No surface gold labeling occurs on apoptotic PMN without primary granule translocation. Original magnifications: (*A* and *B*) ×35,000; (insets *A* and *B*) ×54,000; (*C*) ×12,300; (*D*) ×14,800.

nuclear disintegration that has lost membrane integrity (Fig. 8 *A*, *left*). Labeling was specific for translocation of primary granules, as shown by the virtual absence of labeling for viable PMN (Fig. 8 *C*) or apoptotic PMN that had not undergone primary granule translocation (Fig. 8 *D*).

Discussion

Although ANCA are a highly sensitive and specific marker for Wegener's granulomatosis and microscopic polyarteritis, (1–4), their pathogenic role remains uncertain. The most difficult problem has been to explain how extracellular ANCA interact with intracellular primary granule components. For this reason, most models invoke a "priming" event in which cytoplasmic primary granules translocate to the PMN cell surface (8–10, 13, 14, 28). We show that ANCA Ag are expressed on the surface of apoptotic PMN. Translocation of primary granules occurs as a natural consequence of apoptosis, without priming. Moreover, we show that, once expressed on the surface of apoptotic PMN, primary granule components may interact with circulating ANCA.

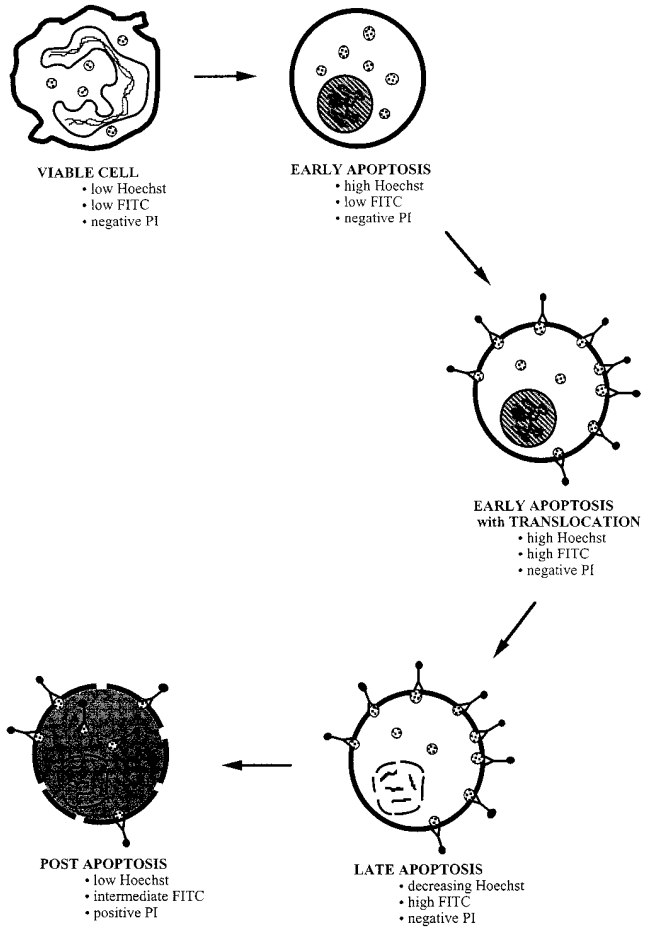

Figure 9. PMN undergoing apoptosis progress through discrete phases. During early apoptosis, nuclear chromatin condenses and nuclear lobes coalesce into a single body. Nucleus disintegration occurs with movement into late apoptosis. Translocation and loss of cytoplasmic primary granules is more distinct during late-phase apoptosis, but also occurs in early apoptotic PMN before nuclear disintegration. ANCA binding correlates with cytoplasmic granular translocation. PMN eventually move into a postapoptotic phase, during which there is loss of cell membrane integrity.

Surface expression of ANCA Ag seems most prominent during the later phases of apoptosis. PMN undergoing apoptosis seem to progress through several discrete phases (Fig. 9). Early apoptotic PMN show most of the classic morphologic features of apoptosis (27). Cells exclude PI and stain brightly with Hoechst dye. PMN moving to a later phase of apoptosis undergo several changes that correlate with surface ANCA recognition. Late apoptotic PMN still exclude PI but show decreased Hoechst staining. EM shows nuclear disintegration and decreased numbers of cytoplasmic granules, many aligned just beneath an intact cell membrane. Although translocation of primary granules is more easily appreciated during later phases of apoptosis, it may also be seen in early apoptotic PMN before nuclear disintegration.

We speculate that, once translocated to the cell surface, cytoplasmic granules are shed in the form of membrane-enclosed apoptotic bodies. This would explain both the decreased number of granules seen by EM in late apoptotic PMN and the marked decrease in total cellular content of ANCA Ag seen by FACS® analysis of postapoptotic PMN. Phagocytic clearance of apoptotic bodies protects tissues from an otherwise harmful exposure to cytoplasmic granular contents (25). Although we cannot exclude the possibility that apoptotic PMN release the contents of their cytoplasmic granules directly into the extracellular space by degranulation, this seems very unlikely. Given the short circulatory half-life of PMN and the large number of PMN released daily by the bone marrow, release of even a fraction of PMN granular contents without phagocytic clearance would produce overwhelming inflammatory injury.

Immunogold labeling confirmed the surface expression of ANCA Ag by apoptotic PMN, but did not identify the structural basis for this expression. Surface labeling was frequently associated with "puffs" extending outward from the cell membrane. Such "puffs" may represent a residual after shedding of granules as apoptotic bodies or even after degranulation. Alternatively, surface expression of ANCA Ag may represent a normal event that is for some reason augmented during apoptosis. Surface expression of lactoferrin (29, 30) and PR3 (30) on normal nonapoptotic PMN has been previously described by immunogold labeling and FACS® analysis.

A major consideration was the potential inadvertent priming of PMN during isolation or overnight culture. However, the data argue sharply against priming as an explanation for our findings. First, isolation of PMN by Ficoll-Hypaque density gradient centrifugation and dextran sedimentation has been shown to yield PMN with a quiescent phenotype (see Materials and Methods) (19–22). Second, freshly isolated PMN incubated with anti-MPO Ab or ANCA sera comprised a single population with low Hoechst and low FITC staining. Third, in PMN cultured to induce apoptosis, surface staining by ANCA sera or anti-MPO Ab was limited to apoptotic PMN. In contrast, surface staining of viable PMN was no different for ANCA-positive vs. ANCA-negative sera. Finally, translocation of cytoplasmic granules was restricted to apoptotic PMN by EM. Viable PMN, displaying morphologic features of mature PMN, showed no translocation. Together, these data indicate that translocation of cytoplasmic granules is specific to the apoptotic process, and not an artifact of PMN isolation and culture.

Our data may have relevance to the pathogenesis of ANCA-related disorders. In most models (8–10, 13, 14), apoptosis could substitute for PMN priming, with ANCA binding to the surface of apoptotic and primed PMN. Recent studies have indicated the importance of the Fc region of ANCA in PMN activation. After binding of ANCA to the cell surface, full activation of PMN seems to depend on binding of ANCA to a second or the same PMN through interaction of ANCA Fc regions with FcγRIIa (CD32) (9, 28, 31, 32). Engagement of β2 integrins may also be a requirement for ANCA-induced activation (28). While it is unclear from these studies whether one or both of the bridged PMN is activated, previous work has shown that engagement of FcγRIIa can mediate PMN activation

(33, 34). In binding of ANCA to the surface of an apoptotic PMN, Fc-dependent bridging could occur via FcγRIIa on a nonapoptotic PMN as in current models (9, 28, 31, 32) or, alternatively, via FcγRIIa on a second or the same apoptotic PMN, since apoptotic PMN have been shown to express normal levels of FcγRIIa (35). We are currently investigating whether apoptotic PMN can be activated by ANCA, either through Ag recognition or FcγRIIa engagement.

Finally, our results may have implications for the initiation of autoimmunity in ANCA-associated disorders. Our data are consistent with growing evidence that apoptotic Ag are the natural targets for many autoAb (24, 36–39). For example, many anti-DNA autoAb seem to be directed against nucleosomal DNA–histone complexes, produced as a result of internucleosomal cleavage during apoptosis. Nucleosomes are a powerful immunogen for autoreactive T cell clones derived from mice with SLE (37). Furthermore, several prominent nuclear and cytoplasmic autoAg targeted in SLE can be found on the surface of apoptotic keratinocytes in the form of either apoptotic bodies or smaller so-called apoptotic blebs (36). These autoAg included nucleosomal DNA, small nuclear ribonucleoproteins, and cytoplasmic RNP (SS-A/Ro, and SS-B/La).

We have recently shown that antiphospholipid Ab from patients with primary antiphospholipid syndrome or SLE recognize the plasma protein β2-glycoprotein I complexed to the surface of apoptotic thymocytes (24). These data and our current demonstration that ANCA Ag can be found on the surface of apoptotic PMN suggest that apoptotic cells may comprise a major source of immunogen in ANCA-associated disorders and autoimmune diseases such as SLE.

The authors are grateful to Dr. John Niles for providing clinical samples and data, and to John Daley for technical assistance in FACS® analysis.

This work was supported by National Institutes of Health grants AR/AI42732 (J.S. Levine), DK44380 (H.R. Brady), and DK45047 (M.A. Shia); a Young Investigator Award from the National Kidney Foundation (J.S. Levine); a Research Unit Grant from the Health Research Board, Ireland (H.R. Brady); The Arthritis Society of Canada (J. Rauch); The Medical Research Council of Canada (J. Rauch); and The Evans Department of Clinical Research, Boston University Medical Center.

Address correspondence to Jerrold S. Levine, Renal Section, E428, Boston University Medical Center Hospital, 88 East Newton Street, Boston, Massachusetts, 02118.

Received for publication 24 June 1996 and in revised form 9 October 1996.

References

1. Van der Woude, F.J., N. Rasmussen, S. Lobatto, A. Wiik, H. Permin, L.A. van Es, M. van der Giessen, G.K. van der Hem, and T.H. The. 1985. Autoantibodies against neutrophils and monocytes. Tools for diagnosis and marker of disease activity in Wegener's granulomatosis. *Lancet. i*:425–429.
2. Falk, R.J., and J.C. Jeannette. 1988. Anti-neutrophil cytoplasmic autoantibodies with specificity for myeloperoxidase in patients with systemic vasculitis and idiopathic necrotizing and crescentic glomerulonephritis. *N. Eng. J. Med.* 318:1651–1657.
3. Nölle, B., U. Specks, J. Lüdemann, M.S. Rohrbach, R.A. DeRemee, and W.L. Gross. 1989. Anticytoplasmic autoantibodies: their immunodiagnostic value in Wegener granulomatosis. *Ann. Int. Med.* 111:28–40.
4. Cohen Tervaert, J.W., R. Goldschmeding, J.D. Elema, P.C. Limburg, M. van der Giessen, M.G. Huitema, M.I. Koolen, R.J. Hené, T.H. The, G.K. van der Hem, et al. 1990. Association of autoantibodies to myeloperoxidase with different forms of vasculitis. *Arthritis Rheum.* 33:1264–1272.
5. Lesavre, P. 1991. Antineutrophil cytoplasmic autoantibodies antigen specificity. *Am. J. Kidney Dis.* 18:159–163.
6. Niles, J.L., R.T. McCluskey, M.F. Ahmad, and M.A. Arnaout. 1989. Wegener's granulomatosis autoantigen is a novel neutrophil serine protease. *Blood.* 74:1888–1893.
7. Charles, L.A., R.J. Falk, and J.C. Jennette. 1989. Reactivity of anti-neutrophil cytoplasmic autoantibodies with HL-60 cells. *Clin. Immunol. Immunopathol.* 53:243–253.
8. Gross, W.L., S. Hauschild, and N. Mistry. 1993. The clinical relevance of ANCA in vasculitis. *Clin. Exp. Immunol.* 93(Suppl. 1): 7–11.
9. Kallenberg, C.G.M., E. Brouwer, A.H.L. Mulder, C.A. Stegeman, J.J. Weening, and J.W. Cohen Tervaert. 1995. ANCA - pathophysiology revisited. *Clin. Exp. Immunol.* 100:1–3.
10. Falk, R.J., R.S. Terrel, L.A. Charles, and J.C. Jennette. 1990. Antineutrophil cytoplasmic antibodies induce neutrophils to degranulate and produce toxic oxygen radicals in vitro. *Proc. Natl. Acad. Sci. USA.* 87:4115–4119.
11. Bender, J.G., L.C. McPhail, and D.E. van Epps. 1983. Exposure of human neutrophils to chemotactic factors potentiates activation of the respiratory burst enzyme. *J. Immunol.* 130: 2316–2323.
12. Falk, R.J., S. Hogan, T.S. Carey, J.C. Jennette, and The Glomerular Disease Collaborative Network. 1990. Clinical course of anti-neutrophil cytoplasmic autoantibody-associated glomerulonephritis and systemic vasculitis. *Ann. Int. Med.* 113:656–663.

13. Charles, L.A., M.L. Caldar, R.J. Falk, R.S. Terrell, and J.C. Jennette. 1992. Antibodies against granule proteins activate neutrophils in vitro. *J. Leukoc. Biol.* 50:539–546.
14. Ewert, B.H., J.C. Jennette, and R.J. Falk. 1992. Antimyeloperoxidase antibodies stimulate neutrophils to damage human endothelial cells. *Kidney Int.* 41:375–383.
15. Savill, J.S., A.H. Wyllie, J.E. Henson, M.J. Walport, P.M. Henson, and C. Haslett. 1989. Macrophage phagocytosis of aging neutrophils in inflammation. Programmed cell death in the neutrophil leads to its recognition by macrophages. *J. Clin. Invest.* 83:865–875.
16. Steller, H. 1995. Mechanisms and genes of cellular suicide. *Science (Wash. DC).* 267:1445–1449.
17. Niles, J.L., P. GuoLi, A.B. Collins, T. Shannon, S. Skates, R. Fienberg, M.A. Arnaout, and R.T. McCluskey. 1991. Antigen-specific radioimmunoassays for anti-neutrophil cytoplasmic antibodies in the diagnosis of rapidly progressive glomerulonephritis. *J. Am. Soc. Nephrol.* 2:27–36.
18. Feinberg, R., E.J. Mark, M. Goodman, R.T. McCluskey, and J. Niles. 1993. Correlation of antineutrophil cytoplasmic antibodies with the extrarenal histopathology of Wegener's (pathergic) granulomatosis and related forms of vasculitis. *Hum. Pathol.* 24:160–168.
19. Takata, S., M. Matsubara, P.G. Allen, P.A. Janmey, C.N. Serhan, and H.R. Brady. 1994. Remodeling of neutrophil phospholipids with 15 (*S*)-hydroxyeicosatetraenoic acid inhibits leukotriene B4–induced neutrophil migration across endothelium. *J. Clin. Invest.* 93:499–508.
20. Brady, H.R., O. Spertini, W. Jiminez, B.M. Brenner, P.A. Marsden, and T.F. Tedder. 1992. Neutrophils, monocytes, and lymphocytes bind to cytokine-activated kidney glomerular endothelial cells through L-selectin (LAM-1) in vitro. *J. Immunol.* 149:2437–2444.
21. Denton, M.D., P.A. Marsden, F.W. Luscinkas, B.M. Brenner, and H.R. Brady. 1991. Cytokine-induced phagocyte adhesion to human mesangial cells: role of CD11b/CD18 integrins and ICAM-1. *Am. J. Physiol.* 261:F1071–F1079.
22. Brady, H., S. Lamas, A. Papayianni, S. Takata, M. Matsubara, and P. Marsden. 1995. Lipoxygenase product formation and cell adhesion during neutrophil-glomerular endothelial cell interaction. *Am. J. Physiol.* 268:F1–F12.
23. Savill, J. 1992. Apoptosis: a mechanism for regulation of the cell complement of inflamed glomeruli. *Kidney Int.* 41:607–612.
24. Price, B.E., J. Rauch, M.A. Shia, M.T. Walsh, W. Lieberthal, H.M. Gilligan, T. O'Laughlin, J.S. Koh, and J.S. Levine. 1996. Antiphospholipid autoantibodies bind to apoptotic, but not viable, thymocytes in a β2-glycoprotein I-dependent manner. *J. Immunol.* 157:2201–2208.
25. Savill, J., V. Fadok, P. Henson, and C. Haslett. 1993. Phagocyte recognition of cells undergoing apoptosis. *Immunol. Today.* 14:131–136.
26. Morris, R.G., A.D. Hargreaves, E. Duvall, and A.H. Wyllie. 1984. Hormone-induced cell death. 2. Surface changes in thymocytes undergoing apoptosis. *Am. J. Pathol.* 115:426–436.
27. Hébert, M.-J., T. Takano, H. Holthöfer, and H.R. Brady. 1996. Sequential morphological events during apoptosis of human neutrophils: modulation by a lipoxygenase-derived eiscosanoids. *J. Immunol.* 157:3105–3115.
28. Reumaux, D., P.J.M. Vossebeld, D. Roos, and A.J. Verhoeven. 1995. Effect of tumor necrosis factor-induced integrin activation on Fcγ receptor II-mediated signal transduction: relevance for activation of neutrophils by anti-proteinase 3 or anti-myeloperoxidase antibodies. *Blood.* 86:3189–3195.
29. Esaguy, N., A.P. Aguas, and M.T. Silva. 1989. High-resolution localization of lactoferrin in human neutrophils: labeling of secondary granules and cell heterogeneity. *J. Leukoc. Biol.* 46:51–62.
30. Csernok, E., J. Lüdemann, W.L. Gross, and D.F. Bainton. 1990. Ultrastructural localization of proteinase 3, the target antigen of anti-cytoplasmic antibodies circulating in Wegener's granulomatosis. *Am. J. Pathol.* 137:1113–1120.
31. Porges, A.J., P.B. Redecha, W.T. Kimberly, E. Csernok, W.L. Gross, and R.P. Kimberly. 1994. Anti-neutrophil cytoplasmic antibodies engage and activate human neutrophils via FcγRIIa. *J. Immunol.* 153:1271–1280.
32. Mulder, A.H., P. Heeringa, E. Brouwer, P.C. Limburg, and C.G.M. Kallenberg. 1994. Activation of granulocytes by anti-neutrophil cytoplasmic antibodies (ANCA): a FcγRII-dependent process. *Clin. Exp. Immunol.* 98:270–278.
33. Huizinga, T.W.J., F. van Kemenade, L. Koenderman, K.M. Dolman. A.E.G. Kr. von dem Borne, P.A.T. Tetteroo, and D. Roos. 1989. The 40-kDa Fcγ receptor (FcRII) on human neutrophils is essential for the IgG-induced respiratory burst and IgG-induced phagocytosis. *J. Immunol.* 142:2365–2369.
34. Brunkhorst, B.A., G. Strohmeier, K. Lazzari, G. Weil, D. Melnick, H.B. Fleit, and E.R. Simons. 1992. Differential roles of FcγRII and FcγRIII in immune complex stimulation of human neutrophils. *J. Immunol.* 267:20659–20666.
35. Dransfield, I., A.-M. Buckle, J.S. Savill, A. McDowall, C. Haslett, and N. Hogg. 1994. Neutrophil apoptosis is associated with a reduction in CD16 (FcγRIII) expression. *J. Immunol.* 153:1254–1262.
36. Casciola-Rosen, L.A., G. Anhalt, and A. Rosen. 1994. Autoantigens targeted in systemic lupus erythematosus are clustered in two populations of surface blebs on apoptotic keratinocytes. *J. Exp. Med.* 179:1317–1330.
37. Mohan, C., S. Adams, V. Stanik, and S.K. Datta. 1993. Nucleosome: a major immunogen for pathogenic autoantibody-inducing T cells of lupus. *J. Exp. Med.* 177:1367–1381.
38. Bell, D.A., and B. Morrison. 1991. The spontaneous apoptotic cell death of normal human lymphocytes in vitro: the release of, and immunoproliferative response to, nucleosomes in vivo. *Immunol. Immunopathol.* 60:13–26.
39. Tax, W.J.M., C. Kramers, M.C.K. van Bruggen, and J.H.M. Berden. 1995. Apoptosis, nucleosomes, and nephritis in systemic lupus erythematosus. *Kidney Int.* 48:666–671.